Dimensionality of Diffusion in Flow-Aligned Surfactant-Templated Mesoporous Silica: A Single Molecule Tracking Study of Pore Wall Permeability

Seok Chan Park, Takashi Ito* and Daniel A. Higgins*
Department of Chemistry, Kansas State University, 213 CBC Building, Manhattan, KS 66506

The chemical structures of the PDI dyes and Pluronic F127 surfactant are given along with a description of the design and fabrication of the microfluidic cell used in these experiments. The detailed procedures employed for distinguishing immobile and mobile molecules and isotropic diffusion from anisotropic diffusion are also given, along with a discussion of the trend analyses and their results. Representative wide-field fluorescence images and corresponding trajectory plots obtained from the silica free F127 gels are provided, along with representative wide-field fluorescence videos acquired from the mesoporous silica samples and F127 gels.

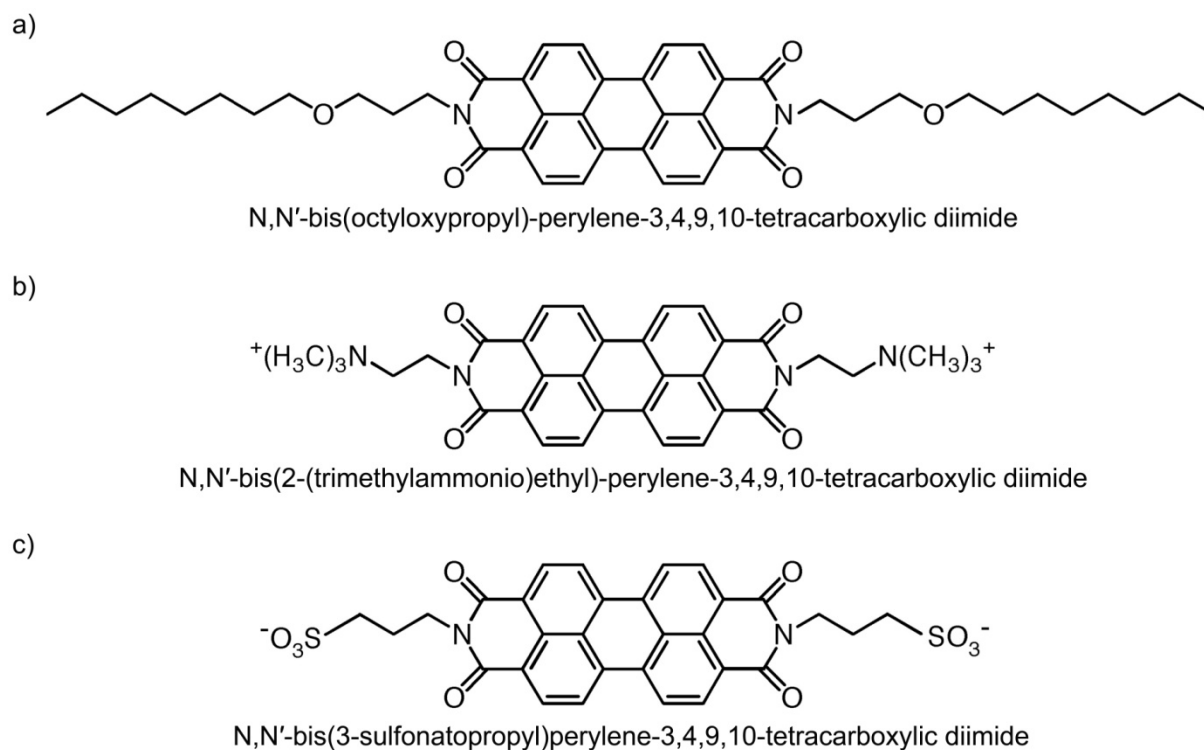*Corresponding author emails: ito@ksu.edu and higgins@ksu.edu

a)

N,N′-bis(octyloxypropyl)-perylene-3,4,9,10-tetracarboxylic diimide

b)

N,N′-bis(2-(trimethylammonio)ethyl)-perylene-3,4,9,10-tetracarboxylic diimide

c)

N,N′-bis(3-sulfonatopropyl)perylene-3,4,9,10-tetracarboxylic diimide

Figure S1. Chemical structures of the uncharged (a), cationic (b), and anionic (c) PDI dye molecules employed in single molecule tracking and FCS experiments.
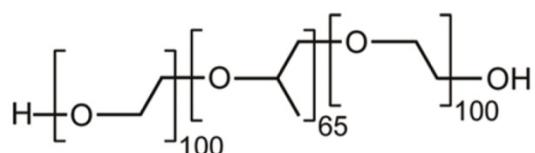

Figure S2. Chemical structure of Pluronic F127.

Fabrication of Microfluidic Channels

Microfluidic channels for flow alignment of the surfactant gels and silica sols (see **Figure S3**) were prepared by casting uncured poly(dimethylsiloxane) (PDMS, Sylgaard 184) in a prefabricated glass mold. A small rectangular piece of glass coverslip was utilized to define the channel dimensions. The channels were designed to be rectangular in shape and of 150 μm

depth, 10 mm length, and 2 mm width. Once cured, the PDMS monolith was removed from the mold, and 1 mm diameter inlet and outlet holes were punched at each end of the channel. The PDMS monolith and a microscope coverslip (FisherFinest Premium) were subsequently cleaned in an air plasma for 30 s and 5 min, respectively, and were then immediately pressed together to form the microfluidic channel. The microscope coverslip formed the bottom surface of the channel. All optical experiments involved imaging through this coverslip.
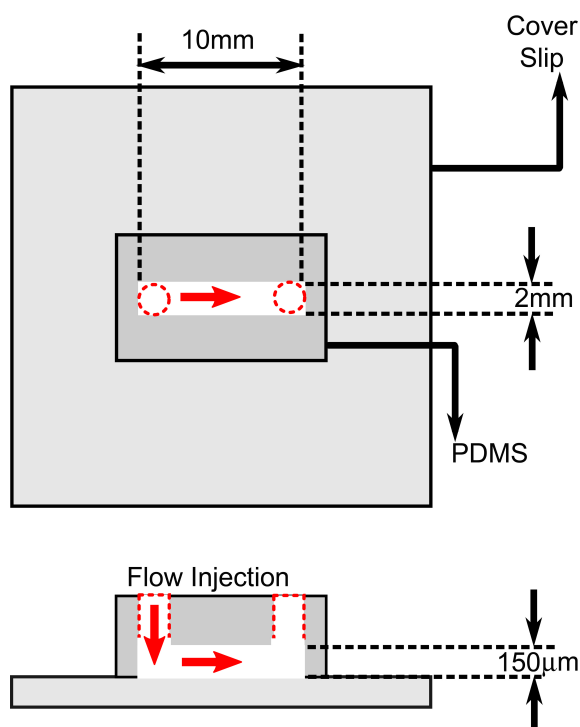

Figure S3. Polydimethylsiloxane-based microfluidic cell employed to obtain flow aligned mesoporous silica monoliths and F127 gels.

Silica sols and surfactant gels were loaded into the channels by first drawing them into a short glass capillary using a syringe pump. The capillary was then contacted to the channel inlet,

and the syringe pump reversed to fill the channel. The viscous sols and gels were flowed into the channels at a linear flow velocity of ~12 mm/min. After filling, the inlet and outlet holes were sealed by covering with another plasma-cleaned coverslip.

Assignment of Molecular Mobility and Diffusion Dimensionality

Assignment of individual molecules to mobile and immobile populations was accomplished by first determining the mean localization precision for the molecules using the following equation:[1]

$$\sigma^2 = \frac{s^2 + a^2/12}{N} + \frac{8\pi s^4 b^2}{a^2 N^2} \tag{S1}$$

Here, σ is the localization precision, s is the Gaussian width of the detected spot, N is the total number of photon counts in the spot area, a is the pixel size and b^2 the background noise, as obtained from the background subtraction step described in Experimental Considerations. The total photon counts were determined as follows:

$$N = 2\pi A s^2 \tag{S2}$$

where the spot amplitude, A, was determined from the Gaussian fit of each spot. The individual molecules were assigned to immobile and mobile fractions by comparing their MSD values to σ^2. Trajectories having MSD $> 4.6\sigma^2$ were classified as mobile, while those with smaller MSD were classified as immobile. This threshold was chosen so that, at most, only ~ 2% of immobile molecules would be mischaracterized as mobile molecules.

The mobile molecules were next separated into 1D and 2D diffusing populations by comparing the σ_δ^2 obtained by orthogonal regression analysis[2] of the trajectory data to σ^2. Trajectories having $\sigma_\delta^2 > 4.6\sigma^2$ were assigned as 2D diffusion and all others as 1D diffusion. Again, this threshold was chosen to limit the misassignment rate to ~ 2%.

The total number of trajectories analyzed in preparing **Figures 2,3** in the main text is given in **Table S1**, while those used for **Figure 4** are given in **Table S2**. The number of time transients used in preparation of **Figure 6** is given in **Table S3.**

Table S1. Total number of trajectories analyzed for **Figures 2,3**, as a function of aging time and dye charge.

	Uncharged	Cationic	Anionic
22 hr	45	89	29
41 hr	50	38	104
77 hr	147	43	109

Table S2. Total number of trajectories analyzed for **Figure 4**, as a function of dye charge and diffusion dimensionality.

	Uncharged	Cationic	Anionic
1D	68	31	105
2D	25	21	163

Table S3. Total number of time transients analyzed for **Figure 6**, as a function of aging time and dye charge.

	Uncharged		Cationic		Anionic	
	1D	3D	1D	3D	1D	3D
22 h	10	10	9	9	10	10
41 h	10	10	10	10	10	9
77 h	6	6	6	6	6	6

Analysis of Trends in SMT and FCS Data

Standard linear least squares methods of trend analysis[3] were employed to assign confidence levels to all trends reported in the main text. In these analyses, the raw data were fit to linear functions to determine the slope, m, and the error on the slope, s_m, for each line. A t-test was then employed to determine the confidence level at which the slope in each case differed from zero. The confidence level reported is for the Student's t-value at which $|m| = t \times s_m$. **Table S4** provides the results of this analysis for the data in **Figure 2** of the main text. **Table S5** provides similar results for the analysis of the data in **Figure 3**, while **Table S6** provides the same information for the data in **Figure 6**. **Table S7** provides the results of a pairwise t-test comparing the diffusion coefficients for molecules exhibiting the same diffusion dimensionality at each aging time, but differing in charge. These results reveal few statistically significant differences in the diffusion coefficients for molecules exhibiting the same diffusion dimensionality at the same aging times. The most significant differences (see **Figure 6)** are observed between molecules exhibiting different diffusion dimensionalities (i.e. 1D vs. 3D).

Table S4. Linear least squares trend analysis of the fractions of 1D and 2D mobile populations for uncharged, cationic and anionic PDI dyes (see **Figure 2**).

	1D				2D			
	Slope $(m)^a$	$s_m{}^b$	$N_f{}^c$	Cl^d	Slope (m)	s_m	N_f	Cl
Uncharged	0.313	0.185	25	90.0%	-0.313	0.185	25	90.0%
Cationic	-0.269	0.201	24	80.0%	0.269	0.201	24	80.0%
Anionic	-0.519	0.205	24	98.0%	0.519	0.205	24	98.0%

[a]Slope of the linear fit. [b]Uncertainty in the slope. [c]Degrees of freedom. [d]Confidence level.

Table S5. Linear least squares trend analysis of the mean trajectory aspect ratios of the 1D and 2D diffusing populations for uncharged, cationic and anionic PDI dyes (see **Figure 3**).

	1D				2D			
	Slope $(m)^a$	$s_m{}^b$	$N_f{}^c$	Cl^d	Slope (m)	s_m	N_f	Cl
Uncharged	0.195	0.020	23	99.9%	0.034	0.009	24	99.9%
Cationic	0.029	0.017	22	80.0%	0.007	0.006	23	70.0%
Anionic	-0.003	0.019	19	50.0%	0.004	0.005	23	60.0%

^{a}Slope of the linear fit. ^{b}Uncertainty in the slope. ^{c}Degrees of freedom. ^{d}Confidence level.

Table S6. Linear least squares trend analysis of diffusion coefficients for the 1D and 3D motions of uncharged, cationic and anionic PDI molecules (see **Figure 6**).

	1D				3D			
	Slope $(m)^a$	$s_m{}^b$	$N_f{}^c$	Cl^d	Slope (m)	s_m	N_f	Cl
Uncharged	-0.153	0.030	24	99.9%	-0.161	0.033	24	99.9%
Cationic	-0.158	0.027	23	99.9%	-0.191	0.041	23	99.9%
Anionic	-0.069	0.021	24	99.5%	-0.150	0.059	23	98.0%

^{a}Slope of the linear fit. ^{b}Uncertainty in the slope. ^{c}Degrees of freedom. ^{d}Confidence level.

Table S7. Pairwise *t*-test results showing the confidence levels at which each pair of FCS-derived diffusion coefficients differ (see **Figure 6**).

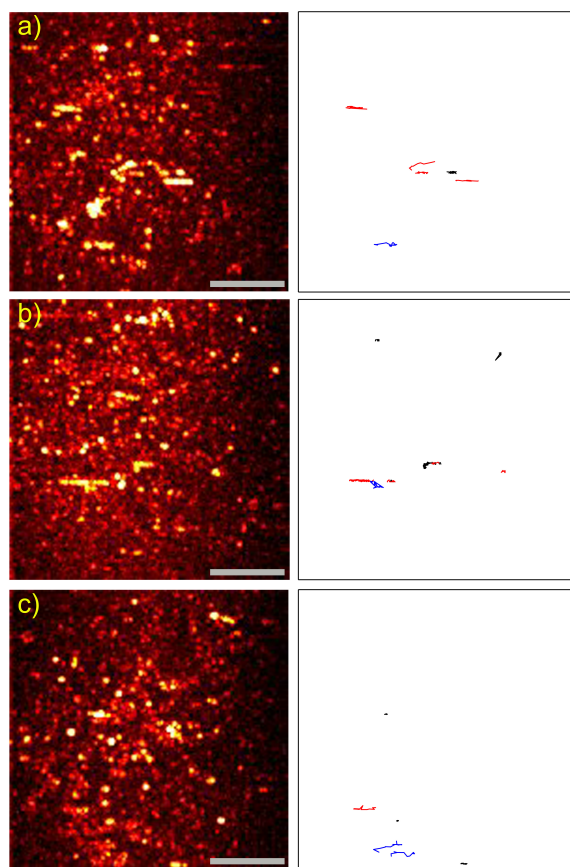|	Uncharged:Cationic		Uncharged:Anionic		Cationic:Anionic	
	1D	3D	1D	3D	1D	3D
22 h	41%	71%	99%	52%	99%	78%
41 h	72%	54%	27%	79%	83%	97%
77 h	66%	15%	29%	59%	45%	65%

Figure S4. Representative TIRF-mode images (left) and corresponding trajectory plots (right) obtained from silica-free F127 gels doped with uncharged (a), cationic (b), and anionic (c) dye. Trajectories (≥ 10 frames in length) obtained by tracking the motions of the molecules were separated into immobile (black), and 1D (red) and 2D (blue) mobile populations. The images were obtained using the Z-project routine in ImageJ and depict the maximum intensity for each pixel in the associated videos. The scale bars are 5 µm in length.

Video S1. Fluorescence video (500 frames, 24 frames/s) depicting uncharged single molecule motion in a flow-aligned mesoporous silica monolith at 22 h aging. The image shown in **Figure 1a** was derived from this video. The pixel size in the video was 125 nm and the total view area of the video is 18.75 µm X 18.75 µm.

Video S2. Fluorescence video (500 frames, 24 frames/s) depicting uncharged single molecule motion in a flow-aligned mesoporous silica monolith at 41 h aging. The image shown in **Figure 1b** was derived from this video.

Video S3. Fluorescence video (500 frames, 24 frames/s) depicting uncharged single molecule motion in a flow-aligned mesoporous silica monolith at 77 h aging. The image shown in **Figure 1c** was derived from this video.

Video S4. Fluorescence video (500 frames, 24 frames/s) depicting cationic single molecule motion in a flow-aligned mesoporous silica monolith at 22 h aging. The image shown in **Figure 1d** was derived from this video.

Video S5. Fluorescence video (500 frames, 24 frames/s) depicting cationic single molecule motion in a flow-aligned mesoporous silica monolith at 41 h aging. The image shown in **Figure 1e** was derived from this video.

Video S6. Fluorescence video (500 frames, 24 frames/s) depicting cationic single molecule motion in a flow-aligned mesoporous silica monolith at 77 h aging. The image shown in **Figure 1f** was derived from this video.

Video S7. Fluorescence video (500 frames, 24 frames/s) depicting anionic single molecule motion in a flow-aligned mesoporous silica monolith at 22 h aging. The image shown in **Figure 1g** was derived from this video.

Video S8. Fluorescence video (500 frames, 24 frames/s) depicting anionic single molecule motion in a flow-aligned mesoporous silica monolith at 41 h aging. The image shown in **Figure 1h** was derived from this video.

Video S9. Fluorescence video (500 frames, 24 frames/s) depicting anionic single molecule motion in a flow-aligned mesoporous silica monolith at 77 h aging. The image shown in **Figure 1i** was derived from this video.

Video S10. Fluorescence video (500 frames, 24 frames/s) depicting single molecule motion of uncharged dye molecules in a flow-aligned silica free F127 gel. The image shown in **Figure S4a** was derived from this video.

Video S11. Fluorescence video (500 frames, 24 frames/s) depicting single molecule motion of cationic dye molecules in the F127 gel. The image shown in **Figure S4b** was derived from this video.

Video S12. Fluorescence video (500 frames, 24 frames/s) depicting single molecule motion of anionic dye molecules in a flow-aligned silica free F127 gel. The image shown in **Figure S4c** was derived from this video.

REFERENCES

(1)   Thompson, R. E.; Larson, D. R.; Webb, W. W. Precise Nanometer Localization Analysis for Individual Fluorescent Probes. *Biophys. J.* **2002**, *82*, 2775-2783.

(2)   Tran Ba, K. H.; Everett, T. A.; Ito, T.; Higgins, D. A. Trajectory Angle Determination in One Dimensional Single Molecule Tracking Data by Orthogonal Regression Analysis. *Phys. Chem. Chem. Phys.* **2011**, *13*, 1827-35.

(3)   Harris, D. C. *Quantitative Chemical Analysis, 8th ed.* W. H. Freeman: New York, 2010; pp. 68-90.